

PAPER • OPEN ACCESS

High potential of yellow potato (*Solanum Tuberosum L.*) peel waste as porous carbon source for supercapacitor electrodes

To cite this article: Dinda Pertiwi *et al* 2022 *J. Phys.: Conf. Ser.* **2193** 012019

View the [article online](#) for updates and enhancements.

You may also like

- [Utilization of banana peel waste for citric acid production by *Aspergillus niger*](#)
K Khairan, A Makstum and C Yulvizar
- [Preparation of Activated Carbons Originated from Orange Peel Waste by Subcritical H₂O Activation Method](#)
Dandy Hady, Ratna Frida Susanti and Arenst Andreas Arie
- [Fabrication of supercapacitor electrode based on pepper peel activated carbon](#)
W B Kurniawan, K Kurniawan and Ipi



The Electrochemical Society
Advancing solid state & electrochemical science & technology

242nd ECS Meeting

Oct 9 – 13, 2022 • Atlanta, GA, US

Abstract submission deadline: **April 8, 2022**

Connect. Engage. Champion. Empower. Accelerate.

MOVE SCIENCE FORWARD



Submit your abstract



High potential of yellow potato (*Solanum Tuberosum L.*) peel waste as porous carbon source for supercapacitor electrodes

Dinda Pertiwi¹, Novi Yanti¹, and Rika Taslim^{2,*}

¹ Department of Physics, Faculty of Mathematic and Natural Sciences, University of Riau, 28293, Panam, Pekanbaru, Indonesia

² Department of Industrial Engineering, State Islamic University Sultan Syarif Kasim Riau, 28293, Panam, Pekanbaru, Indonesia

*rikataslim@gmail.com

Abstract. Yellow potato peel contains chemical components such as protein, fiber, starch and sugar which is composed atom carbon chains bonding. Heating potato peel at high temperatures can disrupt the bonding of the carbon atoms of the constituents, vaporizing volatile compounds, thereby producing high carbon fixed. This study preparation yellow potato peel-based carbon electrodes through a single-stage integrated pyrolysis with carbonization from room temperature to 600 °C in N₂ gas atmosphere followed by physical activation to a temperature of 850°C in CO₂ gas environment. The impregnation of ZnCl₂ at different concentrations was optimized as an independent variable precursor to produce porous activated carbon for energy storage devices. The difference in concentration of 0.1M, 0.3M and 0.5M ZnCl₂ can increase the porosity, structure of amorphous carbon and the resulting high electrochemical performance. Electrochemical properties were characterized using cyclic voltammetry and galvanostatic charge discharge methods in an aqueous electrolyte of 1M H₂SO₄ at a voltage of 0-1000 mV and a scanning rate of 1 mV s⁻¹. Furthermore, the resulting specific capacitance increased from 82.82 F g⁻¹, 195.66 F g⁻¹ and 147.03 F g⁻¹ based on the effect of the concentration of the chemical activator ZnCl₂. While the specific capacitance obtained using the GCD method shows higher numbers, namely 145.13 F g⁻¹, 223.25 F g⁻¹ and 174.08 F g⁻¹. Energy density 27.18 Wh kg⁻¹ and power density 97.93 W kg⁻¹ from cv method. The simple approach of activated carbon from potato peel waste is expected to produce an economical and simple porous carbon electrode for high performance energy storage application.

1. Introduction

The development of energy storage devices in the field of nano carbon has become the focus of interest of researchers in conducting renewable research [1]. Nowadays, an energy storage device with a storage capacity that is superior to capacitors and batteries, a longer life duration, and high durability has been developed, namely the supercapacitor [2,3]. The supercapacitor consists of two symmetrical carbon electrodes, a current collector, an electrolyte and a separator [4]. Its working principle is to store ions from the electrolyte that decomposes in the carbon pores. The smoothness of ion absorption on porous carbon is influenced by the size and distribution of pores on the electrode surface [5,6]. The pore types of activated carbon according to the International Union of Pure and Applied Chemistry (IUPAC), are microporous (< 2 nm), mesoporous (2-50 nm) and macroporous (> 50 nm) [7]. The type



of pore size and distribution make an important contribution to the specific surface area that can increase the storage capacity of the supercapacitor. The surface area of activated carbon reaches the range of 300 - 2000 m² g⁻¹ [8,9]. Many specific surface area studies have been carried out using different biomass such as dried banana leaves 623.5 m² g⁻¹ [10], corn silk 1962.4 m² g⁻¹ [11], and wheat husk 1200 m² g⁻¹ [12,13].

Interestingly, supercapacitors consisting of activated carbon can be made from biomass waste thus that they are more environmentally friendly, economical and provide natural micropores [14,15]. This research focuses on processing potato peel waste into porous activated carbon electrodes for electrical energy storage. Potato is a type of plant that is known throughout the world, because it contains carbohydrates equivalent to white rice but low in calories. In European countries, potatoes are used as a staple food. Potatoes consist of flesh and skin. The flesh of the fruit is processed to be eaten, while the skin is disposed of as waste. The high consumer interest in processed potato-based foods does not only have a positive impact. As happens in potato processing factories, unused potato peels are thrown away as waste. Potato waste that accumulates can pollute the environment such as causing unpleasant odors and clouding the water. Therefore, the researchers innovate to improve the processing of biomass waste, especially potato peels. Potato skins contain crude fiber, sugar, and vitamins which are composed of carbon chain bonds. Potato skins have almost the same chemical content as the fruit, which has 30% - 40% cellulose which can produce carbon when heated to high temperatures.

The addition of several chemical reagents in the processing of carbon electrodes can be used, such as ZnCl₂, KOH, NaOH, K₂CO₃, H₂SO₄, H₃PO₄, and HNO₃ [16–18]. ZnCl₂ activator was selected as chemical reagent this study due to their characteristics as a dehydrating agent, can evaporate completely at a temperature of 756 °C thus initiated optimum micropores [19]. In addition, ZnCl₂ is more environmentally friendly and the price is more economical. The synthesis of porous carbon electrodes is through a single-stage integrated pyrolysis process including carbonization and physical activation [20]. This process was used N₂, Ar, CO₂, and H₂O gases in the furnace tube [21,22]. The process of carbonization and activation is very influential on the formation of pore structures on the carbon electrodes produced based on the amount of volatile compounds and elements other than carbon that evaporate.

In this study, potato peel waste is processed into activated carbon electrodes with high porosity as the electrode based material for supercapacitor. The carbon electrodes were synthesized through ZnCl₂ impregnation in different concentration of 0.1 M, 0.3 M, and 0.5M at high temperature pyrolysis. The carbonization process and physical activation are carried out while maintaining the pore structure and purity of the carbon sample. The physical properties of carbon electrodes were characterized of density of the monolith by measuring the mass, diameter, and thickness of the carbon pellets. The 0.3M ZnCl₂ activated sample confirmed the high capacitive properties of 195.66 F g⁻¹ in the 1 M H₂SO₄ aqueous electrolyte from CV method. These results clearly confirm the potential of potato peel waste as a porous carbon originating material for supercapacitor electrodes. This characterization is to determine the storage capacity of supercapacitor cell electrodes based on potato peel waste with energy density 27.18 Wh kg⁻¹ and power density 97.593 W kg⁻¹ from cv method.

2. Experimental

The synthesis of porous carbon electrodes from potato peel waste (*Solanum Tuberosum L.*) started from the stage of collecting raw materials from a potato chip production house in Pekanbaru. Potato peels with a thickness of < 2 mm were washed using running water until clean. Then, the water content is removed with sunlight and a drying oven at 110 °C. Then, the sample is pre-carbonized in a temperature of 250 °C to brittle the sample, convert it to carbon, and improve its self-adhesiveness. The sample particle refining process was continued using mortar and ball-milling until the size was below 60 μm. The powder samples were chemically activated through ZnCl₂ impregnation with different concentrations of 0.1 M, 0.3 M, and 0.5 M. Furthermore, the sample is minted into the shape of a coin using a high-pressure hydraulic press. Subsequently, it followed by the evaporation of volatile elements of the carbon sample and the opening of the pore structure through the process of

carbonization and physical activation. Carbonization was performed from room temperature to a temperature of 600 °C in N₂ gas atmosphere and physical activation from a temperature of 600 °C to a temperature of 850 °C in CO₂ gas atmosphere. The process of neutralizing the pH of the carbon pellets was continued using distilled water until a sample of pH 7 was obtained to be carried out in the characterization process.

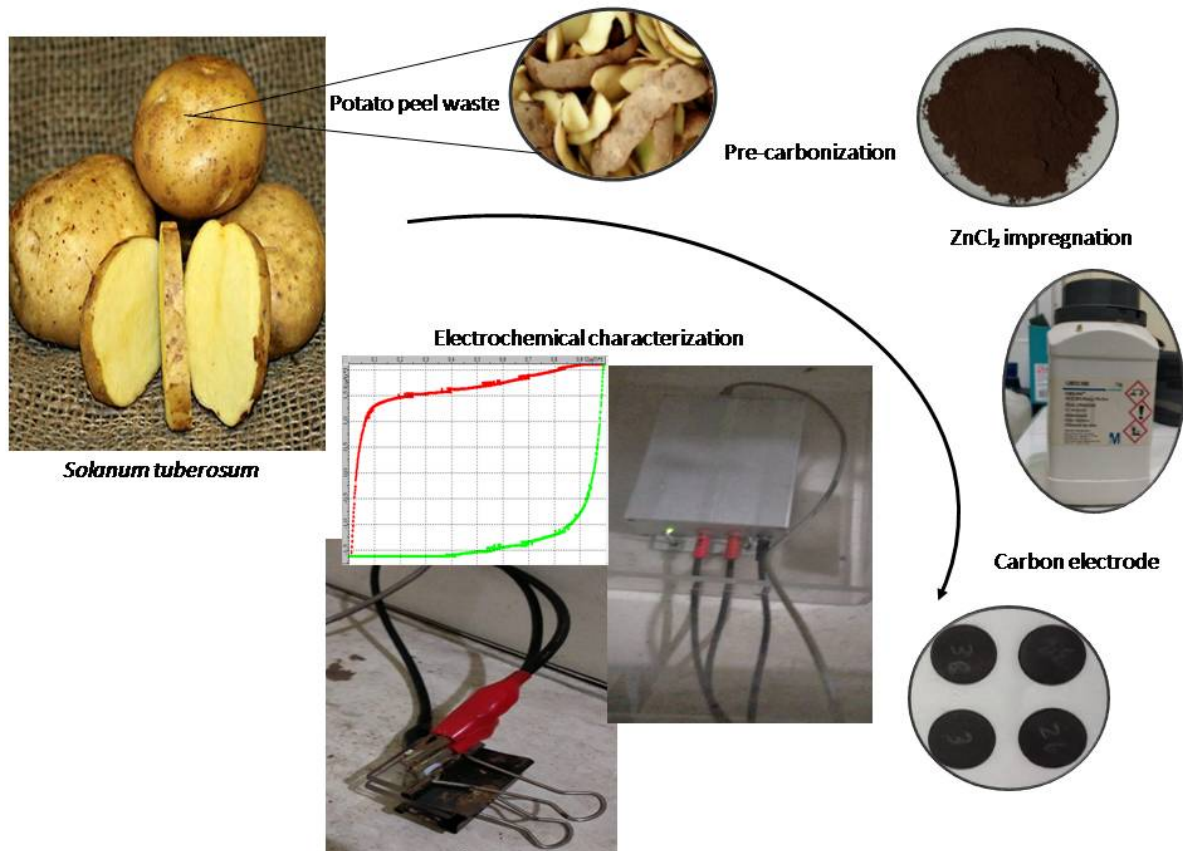


Figure 1. Scheme preparation of *Solanum Tuberosum L* peel-based activated carbon

Carbon electrodes were characterized for their physical properties by calculating the decrease in pellet density after pyrolysis by measuring the mass, diameter, and thickness first. X-ray diffraction characterization was used to determine the degree of crystallinity of carbon samples. Furthermore, cyclic voltamery (CV) and galvanostatic charge discharge (GCD) characterizations were used to determine the storage capacity of the potato peel waste activated carbon electrodes based on their electrochemical properties.

3. Results and Discussions

Density is an initial characterization to determining the physical properties of porous activated carbon electrodes, which is the relationship between the mass and volume of the electrode after pyrolysis [23]. one-stage integrated pyrolysis is a process of heating carbon monolith to a high temperature of up to 900 °C. This process consists of carbonization to a temperature of 600 °C in an N₂ gas environment followed by physical activation to a temperature of 850 °C in a CO₂ gas environment [24]. The carbonization process causes the evaporation of volatile compounds and elements other than carbon in the sample which indicates the creation of empty spaces or pores so that the electrode mass is reduced. Physical activation up to a temperature of 850°C can increase the number and size of existing pores so that high porosity is created [25].

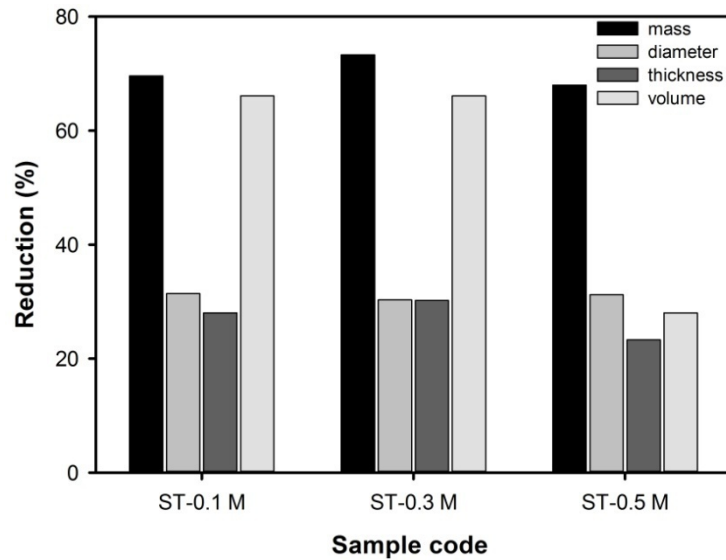


Figure 2. Percentage reduction in mass, diameter and thickness of activated carbon *Solanum Tuberosum L.*

Based on Figure 2, it is known that each variation of the potato peel carbon monolith electrode sample experienced a reduction in mass, diameter and thickness after the pyrolysis process. This reduction causes a decrease in the density value due to evaporation and the addition of porosity. The density reduction for each variation of potato peel waste carbon, as shown in Figure 3.

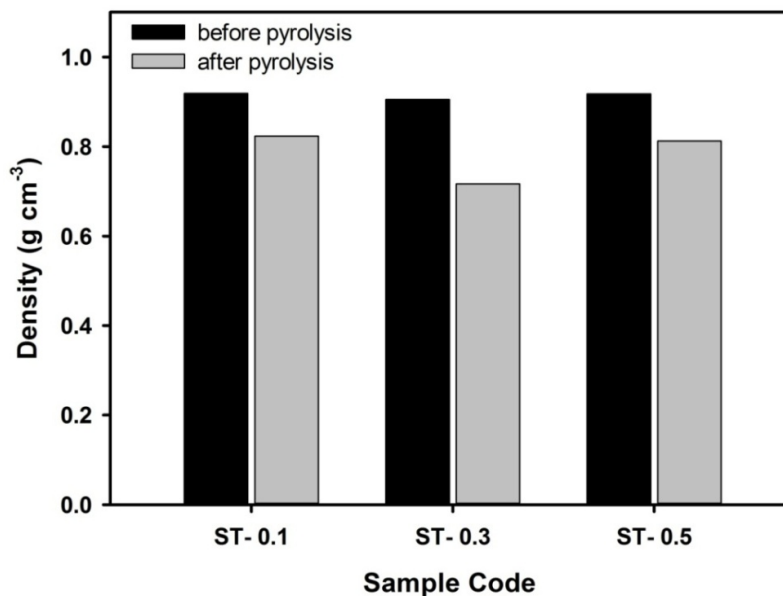


Figure 3. Density decrease of activated carbon *Solanum Tuberosum L.*

Based on Figure 3, it shows the density shrinkage for each variation of the potato peel-based carbon electrode sample. The shrinkage of the sample density of ST-0.1, ST-0.3 and ST-0.5 were 10.38%, 20.86%, and 11.59%, respectively. Density shrinkage is indicated by the release of elements other than carbon that occur during the carbonization process. The elements other than carbon that evaporate during the carbonization process are the natural content of potato skin biomass such as water content and non-carbon elements which are volatile compounds such as cellulose, hemicellulose, and lignin.

Evaporation of elements other than carbon can increase the number of carbon pores, thus that the porosity of the electrode also increases. Density reduction at most does not always contribute positively to the capacitance value, where excessive reduction can disrupt or even damage the carbon chain bonds [26]. The capacitance value is also influenced by the specific surface area of the carbon electrode, the combination of available surface pores such as optimum micropores and mesopores.

X-ray diffraction characterization to determine the degree of crystallinity of carbon samples. This test was carried out at a scattering angle of 2θ showing the 002 and 100 carbon planes in the diffraction angle range of $22^\circ - 25^\circ$ and $42^\circ - 45^\circ$. This test uses a Cu- $k\alpha$ light source which has a wavelength of 1.54 \AA equal to the distance between the lattice in the carbon sample. The test results show a graph with two broad peaks and several sharp peaks which indicated high amorphous carbon dominant [27,28]. These results are almost the same as previous studies using different biomass precursor [29,30]

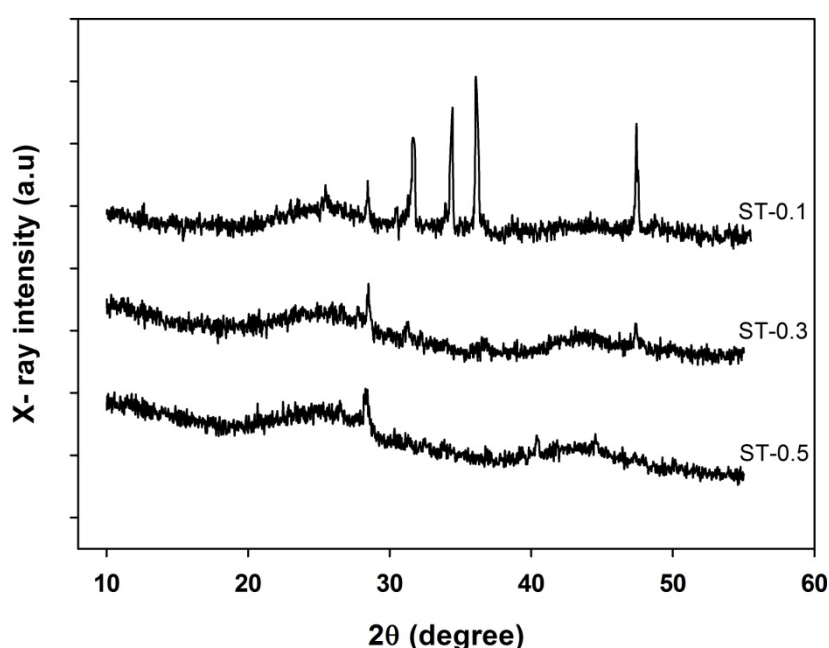


Figure 4. XRD pattern of precursor ST-0.1, ST-0.3 and ST-0.5

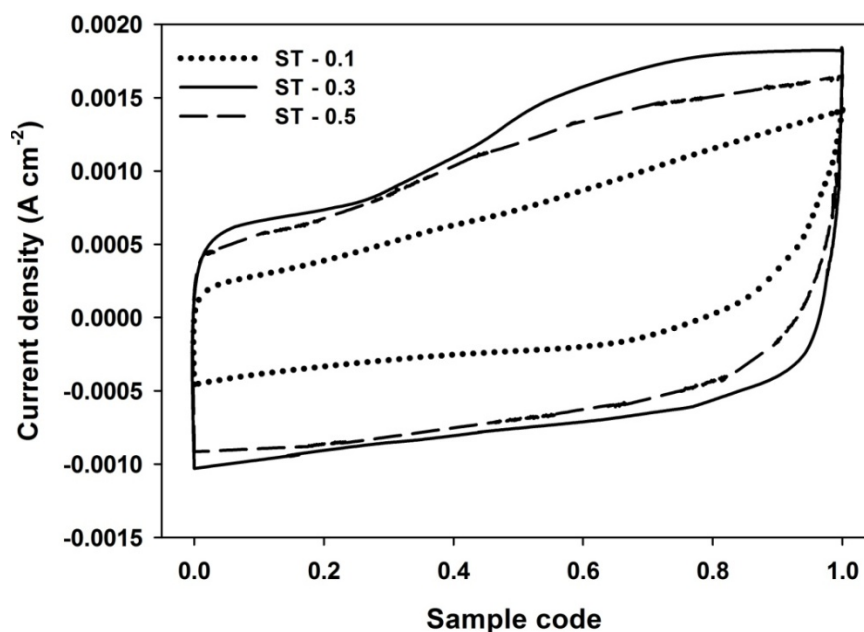
Figure 4 shows the diffraction pattern of potato peel carbon samples based on different concentrations of 0.1M, 0.3M and 0.5M ZnCl_2 activator. The results of the characterization are two sloping peaks that indicate the amorphous nature of the carbon sample. In addition, there are some sharp peaks at several diffraction angles 29° , 34° , 37° and 39° which indicate crystalline properties caused by the presence of elements other than carbon which act as interfering elements [31]. These impurities are compounds such as SiO_2 (JCPDS No. 89-1668), MgO (JCPDS No. 82-1690), and ZnO (JCPDS No. 79-2205).

XRD characterization can be known lattice parameters such as the distance between layers (d_{002} and d_{100}), the height of the microcrystalline layer (L_c) and the width of the microcrystalline layer (L_a) according to Table 1. The lattice parameters were evaluated using Bragg's law and the Debye-Scherrer equation [32]. According to Kumar *et al.* (1999) The value of L_c is inversely proportional to the specific surface area, where the smaller L_c exhibit a large surface area [33,34]. This affects the performance of the electrodes and the storage capacity of the supercapacitor. These results are similar to studies of activated carbon from different biomass [35,36].

Table 1. X-ray diffraction angle, interlayers spacing and microcrystalline dimensions of *Solanum Tuberosum* L. activated carbon

Sample code	$2\theta_{002}$ (°)	$2\theta_{100}$ (°)	d_{002} (Å)	d_{100} (Å)	L_c (Å)	L_a (Å)
ST-0.1	25.754	43.932	3.456	2.059316	19.431	55.400
ST-0.3	25.529	44.634	3.486	2.028543	11.612	19.544
ST-0.5	25.529	44.634	3.486	2.028543	14.149	9.090

CV is the main characterization to determine the performance of supercapacitor cells because it can determine the electrode storage capacity along with its energy density and power density. This characterization is below the potential window of 0 - 1000 mV with a constant scan rate of 1 mV s⁻¹. Carbon electrodes in an aqueous electrolyte of 1 M H₂SO₄ are assembled on a supercapacitor cell body of acrylic material. The symmetrical electrodes are separated by a thin separator to prevent electrical contact. The results of the characterization of this method in the form of a distorted rectangular curve [37,38]. The area of the resulting curve can be a determinant of the capacitance value, where the larger the CV curve area will produce a high capacitance.

**Figure 5.** CV curve of *Solanum Tuberosum* L. activated carbon electrode

Based on Figure 5, the ST-0.3 sample has the largest surface area of the CV curve. This indicates that the ST-0.3 sample has a larger storage capacity than the ST-0.1 and ST-0.5 samples. Based on the CV test, the highest specific capacitance value was obtained in the ST-0.3 sample with a value of 195.03 F g⁻¹. While samples ST-0.1 and ST-0.5 have specific capacitances of 82.82 F g⁻¹ and 147.03 F g⁻¹. The capacitance value increases with the increase in the concentration of ZnCl₂ activator 0.1M to 0.3M which is able to increase the capacitance more than double. Meanwhile, the addition of further activator concentration can disrupt the optimum condition at a concentration of 0.5M so that the capacitance decreases again. The capacitance values obtained from the ST-0.3 and ST-0.5 samples are not too much different. This is due to the pseudocapacitance that can be seen in the CV profile which has an effect on increasing the conductivity of the sample [39,40]. Pseudocapacitance is owned by samples ST-0.3 and ST-0.5 in the highest voltage and inrush current range at ST-0.3. The ST-0.3 sample occurs in a longer voltage range of 0.28 - 0.9 V, while in the ST-0.5 sample occurs in the

0.25 - 0.8 V voltage range. This also causes the ST-0.3 and ST-0.5 samples to have capacitance values that are almost the same and higher than ST-0.1.

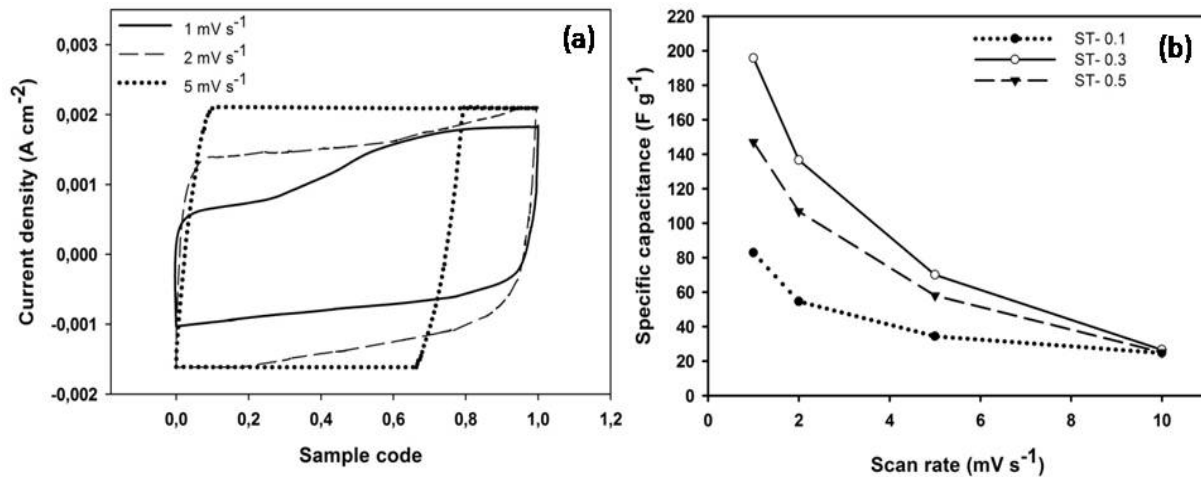


Figure 6. (a) CV curve based on difference in scan rate and (b) Specific capacitance vs. scan rate of all variations

Based on Figures 6 (a) and (b), the scan rate is inversely proportional to the specific capacitance produced. Where a low scan rate of 1 mV s⁻¹ can produce a large capacitance in the supercapacitor. This is due to the low scan rate which takes longer to complete the charge and discharge process. This provides freedom for the dissociated ions to diffuse to fill the carbon pores longer. The optimization of the carbon pore filling certainly gives an increase in the storage capacity of the porous carbon electrodes.

The measurement of electrochemical properties was continued using the Galvanostatic Charge Discharge (GCD) method with a current density of 1 A g⁻¹ and a scan rate of 2 mV s⁻¹. There are three types of GCD measurement curves, namely an isosceles triangle curve which is the ideal type of GCD measurement that shows the EDLC properties of carbon samples. This ideal type indicates that the time required for the charge process is the same as the discharge [41,42]. The second type is an imperfect isosceles triangle which is indicated by a straight vertical line due to internal resistance. The third type is a triangle with one curved side and has internal resistance, where this curved line indicates the presence of a pseudocapacitance due to a surge in the current increase in a certain voltage range [43,44]. The length of time required for the discharge process indicates an increase in the value of the specific capacitance.

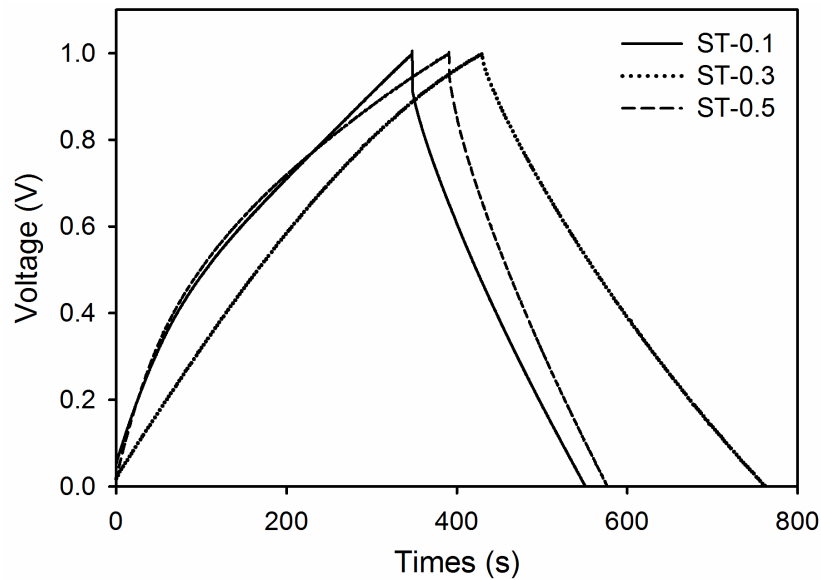


Figure 7. The GCD profile of *Solanum Tuberosum* L.

Based on Figure 7 the difference in capacitance values produced from samples ST-0.1, ST-0.3 and ST-0.5 is influenced by differences in the concentration of the activator given. Where the concentration of activator $ZnCl_2$ 0.3M produces the highest specific capacitance value, namely $223.25 F g^{-1}$ which is indicated by the length of discharge time, the presence of sudocapacitance and internal resistance of potato peel carbon waste samples. While the decrease and increase in concentration from the optimum state can reduce the capacitance value. Where samples ST-0.1 and ST-0.5 have capacitance values of $145.13 F g^{-1}$ and $174.08 F g^{-1}$, respectively. This value confirms a decrease in the thermal resistance of the electrode due to the addition of mesoporous which supports the smooth diffusion of ions [45,46].

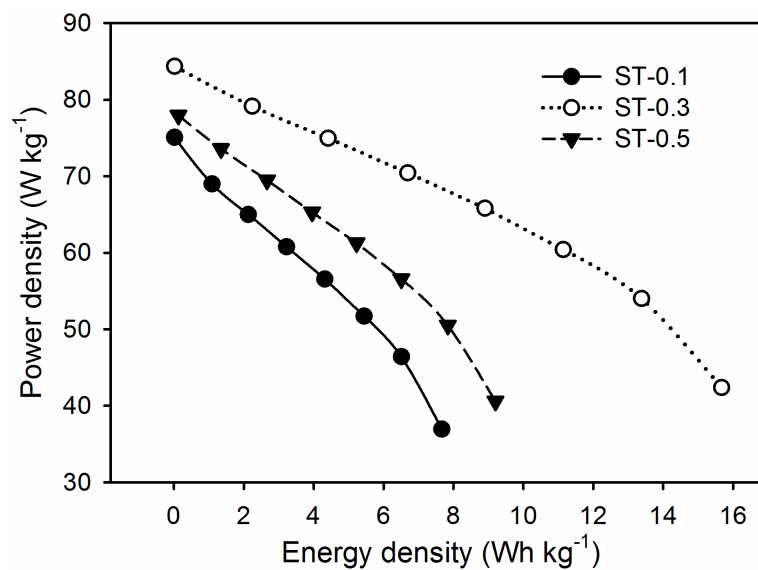


Figure 8. The Ragone of *Solanum Tuberosum* L.

Figure 8 shows a graph of the relationship between energy density and power density measured by the GCD method. Where the sample ST-0.3 has the highest energy density and power density which is influenced by the specific capacitance produced.

4. Conclusion

Potato peel waste has been successfully treated and characterized as the basic material for supercapacitor carbon electrodes. This synthesis that does not require additional adhesives material is an advantage in its processing. Simple and cost-effective methods can increase the use value and sale value of potato peel waste. Different concentrations of ZnCl_2 in chemical activation process can produce different energy storage capacities for each variation. Testing of electrochemical properties using two-electrode system in 1M H_2SO_4 liquid electrolyte at a voltage of 0-1000 mV and a constant scan rate of 1 mV s^{-1} . Different concentrations of ZnCl_2 activator 0.1M, 0.3M and 0.5M can produce the highest specific capacitance at its optimum conditions. Furthermore, the optimum capacitance of supercapacitor from potato peel waste was obtained on sample ST-0.3 ZnCl_2 activator 0.3M with a specific capacitance of 195.66 F g^{-1} , energy density 27.18 Wh kg^{-1} and power density 97.93 W kg^{-1} .

References

- [1] Tyson B M, Abu Al-Rub R K, Yazdanbakhsh A and Grasley Z 2011 Carbon nanotubes and carbon nanofibers for enhancing the mechanical properties of nanocomposite cementitious materials *J. Mater. Civ. Eng.* **23** 1028–35
- [2] Iro Z S, Subramani C and Dash S S 2016 A brief review on electrode materials for supercapacitor *Int. J. Electrochem. Sci.* **11** 10628–43
- [3] González A, Goikolea E, Barrena J A and Mysyk R 2016 Review on supercapacitors: Technologies and materials *Renew. Sustain. Energy Rev.* **58** 1189–206
- [4] Taer E and Taslim R 2018 Brief Review : Preparation Techniques of Biomass Based Activated Carbon Monolith Electrode for Supercapacitor Applications *AIP Conference Proceedings* vol 1927 pp 020004-1-020004-4
- [5] Li X and Wei B 2013 Supercapacitors based on nanostructured carbon *Nano Energy* **2** 159–73
- [6] Gao Z, Zhang Y, Song N and Li X 2017 Biomass-derived renewable carbon materials for electrochemical energy storage *Mater. Res. Lett.* **5** 69–88
- [7] Ayinla R T, Dennis J O, Zaid H M, Sanusi Y K, Usman F and Adebayo L L 2019 A review of technical advances of recent palm bio-waste conversion to activated carbon for energy storage *J. Clean. Prod.* **229** 1427–42
- [8] Poonam, Sharma K, Arora A and Tripathi S K 2019 Review of supercapacitors: Materials and devices *J. Energy Storage* **21** 801–25
- [9] Zheng L, Dai X, Ouyang Y, Chen Y and Wang X 2021 nHighly N/O co-doped carbon nanospheres for symmetric supercapacitors application with high specific energy *J. Energy Storage* **33** 102152
- [10] Apriwandi A, Taer E, Farma R, Setiadi R N and Amiruddin E 2021 A facile approach of micro-mesopores structure binder-free coin/monolith solid design activated carbon for electrode supercapacitor *J. Energy Storage* **40** 102823
- [11] Zhou J, Yuan S, Lu C, Yang M and Song Y 2020 Hierarchical porous carbon microtubes derived from corn silks for supercapacitors electrode materials *J. Electroanal. Chem.* **878** 114704
- [12] Gou G, Huang F, Jiang M, Li J and Zhou Z 2020 Hierarchical porous carbon electrode materials for supercapacitor developed from wheat straw cellulosic foam *Renew. Energy* **149** 208–16
- [13] Yang W, Shi Z, Guo H, Guo J, Lei X and Yue L 2017 Study on preparation of nanocarbon fibers from wheat-straw based on electrostatic spinning method and its application in supercapacitor *Int. J. Electrochem. Sci.* **12** 5587–97
- [14] Gao Y P, Zhai Z B, Huang K J and Zhang Y Y 2017 Energy storage applications of biomass-

- derived carbon materials: Batteries and supercapacitors *New J. Chem.* **41** 11456–70
- [15] Thomas P, Lai C W and Bin Johan M R 2019 Recent developments in biomass-derived carbon as a potential sustainable material for super-capacitor-based energy storage and environmental applications *J. Anal. Appl. Pyrolysis* **140** 54–85
- [16] Boyjoo Y, Cheng Y, Zhong H, Tian H, Pan J, Pareek V K, Jiang S P, Lamoniier J F, Jaroniec M and Liu J 2017 From waste Coca Cola® to activated carbons with impressive capabilities for CO₂ adsorption and supercapacitors *Carbon N. Y.* **116** 490–9
- [17] Mohammed A A, Chen C and Zhu Z 2019 Low-cost, high-performance supercapacitor based on activated carbon electrode materials derived from baobab fruit shells *J. Colloid Interface Sci.* **538** 308–19
- [18] Márquez-Montesino F, Torres-Figueroa N, Lemus-Santana A and Trejo F 2020 Activated Carbon by Potassium Carbonate Activation from Pine Sawdust (*Pinus montezumae* Lamb.) *Chem. Eng. Technol.* **43** 1716–25
- [19] Sun Q, Jiang T, Zhao G and Shi J 2019 Porous carbon material based on biomass prepared by MgO template method and ZnCl₂ activation method as electrode for high performance supercapacitor *Int. J. Electrochem. Sci.* **14** 1–14
- [20] Taer E, Apriwandi A, Taslim R, Malik U and Usman Z 2019 Single Step Carbonization-Activation of Durian Shells for Producing Activated Carbon Monolith Electrodes *Int. J. Electrochem. Sci.* **14** 1318–30
- [21] Miller E E, Hua Y and Tezel F H 2018 Materials for energy storage: Review of electrode materials and methods of increasing capacitance for supercapacitors *J. Energy Storage* **20** 30–40
- [22] Şahin Ö and Saka C 2013 Preparation and characterization of activated carbon from acorn shell by physical activation with H₂O-CO₂ in two-step pretreatment *Bioresour. Technol.* **136** 163–8
- [23] Taer E, Deraman M, Taslim R and Iwantono 2013 Preparation of binderless activated carbon monolith from pre-carbonization rubber wood sawdust by controlling of carbonization and activation condition *AIP Conf. Proc.* **1554** 33–7
- [24] Taer E, Susanti Y, Awitdrus A, Sugianto S, Taslim R, Setiadi R N, Bahri S, Agustino A, Dewi P and Kurniasih B 2018 The effect of CO₂ activation temperature on the physical and electrochemical properties of activated carbon monolith from banana stem waste *AIP Conf. Proc.* **1927** 030016–1–030016–5
- [25] Deraman M, Ishak M M, Farma R, Awitdrus, Taer E, Talib I A and Omar R 2011 Binderless composite electrode monolith from carbon nanotube and biomass carbon activated by H₂SO₄ and CO₂ gas for supercapacitor *AIP Conf. Proc.* **1415** 175–9
- [26] Taer E, Handayani R, Apriwandi A, Taslim R, Awitdrus, Amri A, Agustino and Iwantono I 2019 The Synthesis of Bridging Carbon Particles with Carbon Nanotubes from Areca catechu Husk Waste as Supercapacitor Electrodes *Int. J. Electrochem. Sci.* **14** 9436–48
- [27] Pourhosseini S E M, Norouzi O and Naderi H R 2017 Study of micro/macro ordered porous carbon with olive-shaped structure derived from *Cladophora glomerata* macroalgae as efficient working electrodes of supercapacitors *Biomass and Bioenergy* **107** 287–98
- [28] Song M, Jin B, Xiao R, Yang L, Wu Y, Zhong Z and Huang Y 2013 The comparison of two activation techniques to prepare activated carbon from corn cob *Biomass and Bioenergy* **48** 250–6
- [29] Lu W, Cao X, Hao L, Zhou Y and Wang Y 2020 Activated carbon derived from pitaya peel for supercapacitor applications with high capacitance performance *Mater. Lett.* **264** 127339
- [30] Li Y, Wang X and Cao M 2018 Three-dimensional porous carbon frameworks derived from mangosteen peel waste as promising materials for CO₂ capture and supercapacitors *J. CO₂ Util.* **27** 204–16
- [31] Taer E, Apriwandi, Dalimunthe B K L and Taslim R 2021 A rod-like mesoporous carbon derived from agro-industrial cassava petiole waste for supercapacitor application *J. Chem.*

Technol. Biotechnol. **96**

- [32] Serafin J, Baca M, Biegun M, Mijowska E, Kaleńczuk R J, Sreńscek-Nazzal J and Michalkiewicz B 2019 Direct conversion of biomass to nanoporous activated biocarbons for high CO₂ adsorption and supercapacitor applications *Appl. Surf. Sci.* **497** 143722
- [33] Kumar K, Saxena R K, Kothari R, Suri D K, Kaushik N K and Bohra J N 1997 Correlation between adsorption and x-ray diffraction studies on viscose rayon based activated carbon cloth *Carbon N. Y.* **35** 1842–4
- [34] Deraman M, Daik R, Soltaninejad S, Nor N S M, Awitdrus, Farma R, Mamat N F, Basri N H and Othman M A R 2015 A New Empirical Equation for Estimating Specific Surface Area of Supercapacitor Carbon Electrode from X-Ray Diffraction *Adv. Mater. Res.* **1108** 1–7
- [35] Taslim R, Dewi T R, Taer E, Apriwandi A, Agustino A and Setiadi R N 2018 Effect of physical activation time on the preparation of carbon electrodes from pineapple crown waste for supercapacitor application *J. Phys. Conf. Ser.* **1120** 012084
- [36] Taer E, Afrianda A, Taslim R, Krisman, Minarni, Agustino A, Apriwandi A and Malik U 2018 The physical and electrochemical properties of activated carbon electrode made from Terminalia Catappa leaf (TCL) for supercapacitor cell application *J. Phys. Conf. Ser.* **1120** 012007
- [37] Hor A A and Hashmi S A 2020 Optimization of hierarchical porous carbon derived from a biomass pollen-cone as high-performance electrodes for supercapacitors *Electrochim. Acta* **356** 136826
- [38] Shu Y, Bai Q, Fu G, Xiong Q, Li C, Ding H, Shen Y and Uyama H 2020 Hierarchical porous carbons from polysaccharides carboxymethyl cellulose, bacterial cellulose, and citric acid for supercapacitor *Carbohydr. Polym.* **227** 115346
- [39] Ma Y, Zhang X, Liang Z, Wang C and Sui Y 2020 B/P/N/O co-doped hierarchical porous carbon nano fiber self-standing film with high volumetric and gravimetric capacitance performances for aqueous supercapacitors *Electrochim. Acta* **337** 135800
- [40] Zhao Y P, Xu R X, Cao J P, Zhang X Y, Zhu J S and Wei X Y 2020 N/O co-doped interlinked porous carbon nanoflakes derived from soybean stalk for high-performance supercapacitors *J. Electroanal. Chem.* **871** 114288
- [41] Yao Y, Chen X, Yu N, Wei F and Feng H 2018 Preparation and Supercapacitive Performance of Lead Dioxide Electrodes with Three-Dimensional Porous Structure *Russ. J. Electrochem.* **54** 585–91
- [42] Inal I I G, Holmes S M, Banford A and Aktas Z 2015 The performance of supercapacitor electrodes developed from chemically activated carbon produced from waste tea *Appl. Surf. Sci.* **357** 696–703
- [43] Chen M, Yu D, Zheng X and Dong X 2019 Biomass based N-doped hierarchical porous carbon nanosheets for all-solid-state supercapacitors *J. Energy Storage* **21** 105–12
- [44] Dong X L, Lu A H, He B and Li W C 2016 Highly microporous carbons derived from a complex of glutamic acid and zinc chloride for use in supercapacitors *J. Power Sources* **327** 535–42
- [45] Liu F, Wang Z, Zhang H, Jin L, Chu X, Gu B, Huang H and Yang W 2019 Nitrogen, oxygen and sulfur co-doped hierarchical porous carbons toward high-performance supercapacitors by direct pyrolysis of kraft lignin *Carbon N. Y.* **149** 105–16
- [46] Taer E, Pratiwi L, Apriwandi, Mustika W S, Taslim R and Agustino 2020 Three-dimensional pore structure of activated carbon monolithic derived from hierarchically bamboo stem for supercapacitor application *Commun. Sci. Technol.* **5** 22–30